

Distribution of Actinomycetes in Suez Gulf (Egypt) and Optimization of the Nanoparticles Production of Some Isolates

Gehan M. Abou-elela¹, Hanan M. Abd-Elnaby¹, Usama Abd-Elraouf² and Moaz. M. Hamed^{1,*}

¹ Marine Microbiology Lab., Marine Environ. Div., National Institute of Oceanography and Fisheries, Egypt.

² Microbiology Lab., Faculty of Science, Al-Azhar University – Assuit Branch, Egypt.

Received: 23 Feb. 2018, Revised: 22 Apr. 2018, Accepted: 27 Apr. 2018.

Published online: 1 May 2018.

Abstract: Sediment samples were collected from the shallow areas of the Suez Gulf during winter 2014. Eight locations were selected for this study included El-Tour, RasSidr, Suez North, Suez Middle, AdabiaHarbour, Ain Sokhna, RasGharib and RasShokheir. The physico- chemical characters of the samples were determined. The highest count of the actinomycetes recorded in Adabia harbor (22cfu/gm) and the lowest count recorded in Ain sokhna station (6cfu/gm). Out of 41 actinomycetes isolates, only 11 isolates showed antimicrobial activities against the bacterial pathogens *Bacillus subtilis* 6633, *Staphylococcus aureus* 25923, *Pseudomonas aeruginosa* 902, *Bacillus cereus*, *Salmonella typhimurium* 14028, *Escherichia coli* 19404, and *Vibrio damsela*. Two isolates identified by molecular techniques as *Streptomyces rochei* HMM13 and *Streptomyces* sp., these two isolates were able to produce gold (0.035, 0.013), silver (0.376, 0.355) and zinc (4.080) nanoparticles. Plackett-Burman Design were applied for optimizing the production of nanoparticles by *Streptomyces rochei* HMM13 against *S. typhimurium* 14028, *E-coli* 19404 and *Vibrio damsela*. The productivity increased by 1.16, 1.13 and 1.32 fold, respectively.

Keywords: Actinomycetes, Nanoparticles, Antimicrobial activity, Plackett- burman design, Optimization, characterization, green synthesis.

1 Introduction

Marine environments present an invaluable source of new natural products that may hold important leads for future drug discovery and development [1,2]. These environments are still in their infancy for isolation of new microbes that can produce pharmaceutically valuable metabolites [3,4].

Actinomycetes are Gram-positive filamentous spore formers with high G+C (>55%) content of DNA. They are free living saprophytic bacteria forming a major group of soil population. *Actinobacteria* are widely distributed in terrestrial and aquatic ecosystems, especially in soil [5]. Around 23,000 bioactive secondary metabolites produced by microorganisms have been reported and actinomycetes alone produce 10,000 of these compounds. Many of these secondary metabolites are potent antibiotics, which has made *Streptomyces* the primary antibiotic-producing organisms exploited by the pharmaceutical industry [6].

The reduction of metal ions using biological systems leads to the formation of size controlled, stable, and dispersed nanoparticles, which possesses attractive physicochemical properties [7, 8]. Biosynthesis of nanoparticles as the name

indicates help in the synthesis of very complex reaction within a fraction of minutes have now taken up the attention towards synthesis grievance the need of environmentally benign technologies in material science [9]. The biosynthesis of nanoparticles by microorganism is a green and eco-friendly technology [10].

Actinomycetes are efficient candidates for metal nanoparticles production extracellularly and intracellularly. The synthesis of nanoparticles by actinomycetes presents good stability and polydispersity. Also, actinomycetes possess important biocidal activity against different pathogens [11, 12].

Optimization of the growth conditions, such as media components, pH, temperature, substrate concentration and inoculum size will not only support the growth but also enhance the productivity and monitor the rate of enzyme activity which affects the synthesis of nanoparticles [11]. Therefore, the present preliminary study was aimed to evaluate the distribution of marine actinomycetes in sediment of Suez-Gulf, Egypt, and optimize the culture conditions using Plackett–Burman Design to enhance the production of nanoparticles by some isolates.

*Corresponding author e-mail: Moaz-Micro@hotmail.com

2 Materials and Methods

2.1 Sampling Sites

Sediment samples were collected from the shallow areas of the Suez Gulf during winter, 2014. The eight locations selected for this study included El-Tour, Ras Sidr, Suez North, Suez Middle, Adabia Harbour, Ain Sokhna, Ras Gharib and Ras Shokheir. They are distributed along the Suez Gulf as shown in (Figure 1). Samples were immediately transported to the laboratory in an ice box for bacteriological analysis which was always completed within 24 h [13].

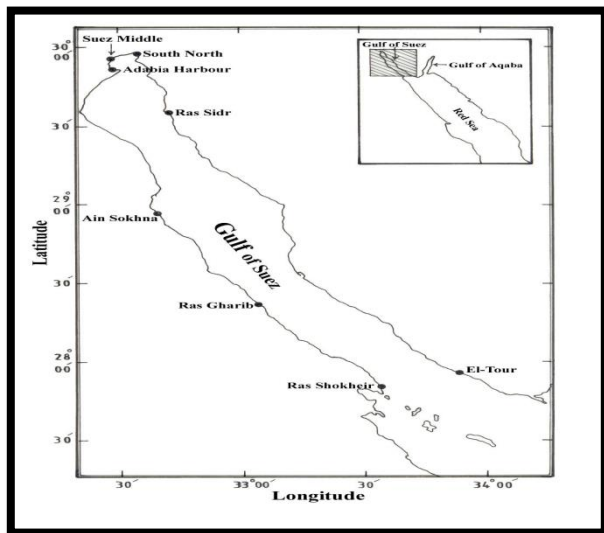


Fig. 1: Sampling sites along the Suez Gulf

2.2 Actinomycetes Isolation and Enumeration

The sediment samples were collected from the shallow areas of the Suez Gulf at depth (0-10 cm). The collected sediment samples were stored in ice box and then transported to the laboratory for bacteriological analysis which completed within 24 h [13]. A suspension of sediment samples was prepared by taken 10g from each sample and then added to 30 ml sterilized sea water, shaken for 20 min. Starch nitrate agar medium was provided with 75 and 25 $\mu\text{g ml}^{-1}$ of filter sterilized cycloheximide and nystatin respectively to minimize fungal contamination. All plates inoculated with 1 ml of the suspension. A triplicate set of dishes was used incubated for 7 days at 32 °C [14].

2.3 Physicochemical Characterization of Sediment Samples

Physical parameters as temperature, pH and salinity were measured in sediment samples. Also chemical characters as dissolved oxygen [15], dissolved phosphate [16], dissolved nitrate [17], dissolved nitrite [16], dissolved ammonia [18]

and organic matter [19] were measured using standard methods.

2.4 Preparation of Cell Free Microbial Extract

The culture medium was prepared, sterilized and inoculated with fresh culture of the actinomycetes isolates. The cultured flasks were incubated at 32 °C for 7 days. After incubation time the cultures were centrifuged at 12000 rpm and their supernatant was used for further experiments [20].

2.4.1 Biological Synthesis of Nanoparticles by Actinomycetes Isolates

2.4.2 Biosynthesis of Silver Nanoparticles (AgNPs)

Each supernatant from actinomycetes isolates were challenged with 0.5-2.0 mM silver nitrate (AgNO_3) with (pH 6.5 – 9.5) as precursor and the flasks were incubated at 37 °C in a shaker under dark condition and observed for color change. The reduction of Ag^+ ions was monitored by sampling an aliquot (2 ml) of the solution at intervals of 24 h and measuring the UV-Vis spectra in range of 300 to 650 nm by using UV-Vis spectrophotometer (Double Beam Spectrophotometer 6800 JENWAY) of the solution [21].

2.4.3 Biosynthesis of Gold Nanoparticles (AuNPs)

Typical reaction mixtures contained equal volumes of actinomycetes supernatant and 0.5, 0.1 and 2.0 mM from chloroauric acid solution (HAuCl_4). The reaction mixtures were incubated at room temperature for 4 h in dark condition. The effect of pH on AuNPs synthesis was studied by adjusting pH of reaction mixture to 2, 3, 4 and 5. Control experiments were conducted with uninoculated media, to check for the role of bacteria in the synthesis of nanoparticles. The absorption spectrum of AuNPs was determined in range of 200-700 nm by using UV-Vis spectrophotometer (Double Beam Spectrophotometer 6800 JENWAY) [22].

2.4.4 Biosynthesis of Zinc Nanoparticles (ZnNPs)

Actinomycetes supernatant was added separately to the reaction vessel containing (50, 100 and 150) mM zinc sulfate solution (v/v). The reaction was carried out in light conditions for 24 h, at 37 °C, pH: (4-7) in rotary shaker with 120 rpm. Supernatant is further used for UV-Visible spectrum by UV-Vis spectrophotometer (Double Beam Spectrophotometer 6800 JENWAY) between 300 to 600 nm at room temperature [23].

2.5 Antimicrobial Assay for Biosynthesized Nanoparticles

Antimicrobial activity of biosynthesized nanoparticles was analyzed for comparative study using agar well diffusion method. The used bacterial indicators were *Bacillus subtilis* 6633, *Staphylococcus aureus* 25923, *Pseudomonas aeruginosa* 9027, *Bacillus cereus*, *Salmonella typhimurium* 14028, *Escherichia coli* 19404 and *Vibrio damsela*. 100 µl of biosynthesized nanoparticles were used as a test sample against the pathogens [21].

2.6 Characterization of Silver Nanoparticles

2.6.1 UV-Visible Spectroscopy Analysis

A small aliquot was drawn from the reaction mixture and a spectrum was taken on a wavelength from 300-600nm on UV-Vis spectrophotometer (Double Beam Spectrophotometer 6800 JENWAY). The reduction of metallic Ag⁺ ions was monitored by measuring the UV-Vis spectrum after reaction. [24].

2.6.2 X-ray Microanalysis

50 µl of the nanoparticles samples were fixed on the specimen stubs and then the samples were examined under x-ray microanalyzer (Module Oxford 6587 INCA x-sigh) attached to JEOL JSM-5500LV scanning electron microscopy at 20 KeV after gold coating using SPI-Module sputter coater [25].

2.6.3 Fourier Transform-Infrared Spectroscopy (FTIR)

A known weight of sample (1 mg) was taken in a mortar and pestle and ground with 2.5 mg of dry potassium bromide (KBr). The samples were scanned using infrared in the range of 4000 to 400/cm using Fourier Transform Infrared Spectrometer. The spectral data obtained were compared with the reference chart to identify the functional groups present in the sample [26].

2.6.4 Scanning Electron Microscopy (SEM)

Scanning electron microscopy (SEM) was used to observe the size, shape and morphology of the resultant nanoparticles. A specimen for SEM sample was made by casting a drop of suspension on a carbon-coated copper grid and the excess solution was removed by tissue paper and allowed to air dry at room temperature [26].

2.7 Identification of the Most Potent Strain

The promising actinomycetes' isolate was cultured in starch-nitrate liquid medium for seven days and genomic DNAs were extracted with the genomic DNA extraction

protocol of Gene Jet genomic DNA purification Kit (Fermentas). Polymerase chain reaction (PCR) using Maxima Hot Start PCR Master Mix (Fermentas). The amplifications were carried out in a thermal cyclor (Multigene Optimax, Labnet international, Inc). The PCR thermocycler was programmed as follow: 95°C for 5 min for initial denaturation, 30 cycles at 95°C for 1 min, 55 °C for 1 min, 72 °C for 2 min and a final extension at 72 °C for 10min. The PCR mixture contained 25 pmol of each primer, 10 ng chromosomal DNA, 200 mmol/L dNTPs and 2.5 U of Taq Polymerase in 50 µL of Taq polymerase buffer 10X Standard Taq Reaction Buffer. The PCR Clean-Up of the PCR product was performed by using Gene JET™ PCR Purification Kit (Fermentas) at Sigma Scientific Services Company, Egypt, 2013. The sequencing of the PCR product was made by the GATC Company by using ABI 3730xl DNA sequence with universal primers (16S_{27F} and 16S1492R), (5'AGAGTTTGATCCTGGCTCAG-3' and 5'-GGTTACCTTGTTACGACTT-3').

Genotypic characterization was performed using 16S sequence analysis. Multiple alignments with sequences of the most closely related members and calculations of levels of sequence similarity were carried out using BioEdit (software version 7) [27]. Sequences of rRNA genes, for comparison, were obtained from the National Center for Biotechnology Information (NCBI) database.

2.8 Enhancement of the Silver Nanoparticles Production by the Most Potent Isolate

2.8.1 Plackett-Burman Design

The Plackett-Burman experimental design [28] was used to evaluate the relative importance of various factors involved in the production of silver nanoparticles by the selected actinomycetes isolate. The independent variables examined in this experiment and their settings are shown in (Table 1). Seven variables shown in (Table 2) were used. The rows in Table 2 represent the 8 different experiments (row no. 9 represents the basal control trial) and each column represents a different variable. For each nutrient variable, a high (+) or low (-) concentration was tested. The main effect of each variable was determined with the following equation:

$$E_{xi} = (\sum M_{i+} - \sum M_{i-}) / N$$

Where E_{xi} is the variable main effect, M_{i+} and M_{i-} are the radius of the clear zone around each well in the trials. The independent variable (xi) was present in the high and low concentrations, respectively, and N is the number of trials divided by 2. Using Microsoft Excel, statistical t-values for equal unpaired samples were calculated according to Cochran and Snedecor [29] using Microsoft excels to determine the variable significance. From main effect results an optimized medium was predicted.

Verification Experiment: A verification experiment was carried out in duplicates, the predicted optimum levels of the independent variables were examined and compared to the basal conditions setting and the average production of the secondary metabolites was calculated.

Table 1: Independent variables affecting antimicrobial agent(s) production

Factor	Symbol	Level		
		-1	0	+1
Starch (g/l)	Starch	10	20	30
KNO ₃ (g/l)	KN	0.5	1.0	1.5
K ₂ HPO ₄ (g/l)	K ₂	0.25	0.5	0.75
MgSO ₄ .7H ₂ O(g/l)	Mg	0.25	0.5	0.75
FeSO ₄ (g/l)	Fe	0.005	0.01	0.015
Temperature	Temp	33	35	37
pH	pH	6	7	8

3

* Inoculum size was added in ml of 7 days culture filtrate (10^3 CFU/ml).

Table 2: The Plackett-Burman experimental design for 7 factors

Trials	St	KN	K ₂	Mg	Fe	pH	Temp
1	-	-	-	+	+	+	-
2	+	-	-	-	-	+	+
3	-	+	-	-	+	-	+
4	+	+	-	+	-	-	-
5	-	-	+	+	-	-	+
6	+	-	+	-	+	-	-
7	-	+	+	-	-	+	-
8	+	+	+	+	+	+	+
9	0	0	0	0	0	0	0

3 Results and Discussion

3.1 Physical and Chemical Characters of Sediment Samples

Sediment samples collected in winter, 2014 from different along Sues Gulf were analyzed for physical and chemical properties. The data in Table 3 indicates that, temperature ranged from 17.6 °C in Suez North to 19.6°C in El-Tour ,this may be due to several factors such as, air temperature and winds in this time of year. Hamed [30]stated that, temperature of surface water in the Gulf of Suez ranged between 16.5°C to 19.5 °C during winter. The pH values showed tendency toward alkalinity (>8).The pH of seawater is relatively constant due to the presence of carbonate, bicarbonate ions and varied from 7.8 to 8.3 in polluted water it falls outside this range [31].Sediment samples exhibited pH range from 8.14 to 8.25. Salinity values of samples

ranged from 40.2‰ in El-Tour to 41.9‰ in Suez Middle. The chemical parameters including dissolved phosphate, nitrate, nitrite, ammonia and organic matter varied according to the sampling sites as shown in (Table 3).The highest dissolved phosphate in samples was shown at Ras Gharib site (3.88 µg at.PO₄-P/l), while the lowest concentration of phosphate at Ain Sokhna site (0.14 µg at.PO₄-P/l) an observation previously reported by Fahmy *et al.*[32] attributed this to the flourishing of phytoplankton which consumes this element.Organic matter in samples showed the highest value at RasGharib (7.12 mg/l), while the lowest value showed at Ain Sokhna (0.71 mg/l) with low population density at that time of the year.Nitrate level showed more or less comparable values which ranged from 0.12 µg at.NO₃-N/l at RasShokair site to 45.61 µg at.NO₃-N/lat Suez Middle site.These results may be due to discharge of sewage wastes of nitrate from bottom sediments into overlying water. According to WHO [33]the nitrite existence in water sources due to fertilizer use decayed vegetable and animal matter, domestic effluents, sewage sludge disposal to land, industrial discharges, and leaches from refuse dumps and atmospheric washout. Dissolved nitrite measured in samples revealed a high value (2.22 µg at. NO₂-N/l) in samples of RasGharib site compared to other sampling sites and that results agree with Hamed [30]whostudied the surface concentration of nitrite in the Gulf of Suez and northern part of the Red Sea and he found that, the maximum concentration was 0.47 µmol/L during winter at RasAdabiya while the low concentration was recorded at Gafton station during summer (0.02 µmol/L). Ammonia concentration at RasGharib site was the much higher (47.2 µg at. NH₃-N/l) and El-Tour site recorded the much lower (0.3µg at. NH₃-N/l). Such concentration of ammonia is an indicator of the presence of pollutants of high activity and this is may be attributed to human activities of diverse origin and presence of water treatment planned of wastewater of RasGharib near these station, these results disagreed with that of Hamed[30]who reported that, the maximum surface ammonia concentration was 6.86 µmol/L during winter at RasAdabiya.

3.2 Actinomycetes Viable Counts in Sediment Samples

The actinomycetes count was represented as colony forming unit (CFU/gm) for sediment samples. As shown in (Table 4), the highest count of actinomycetes recoded in AdabiaHarbour Station (22 CFU /gm), while the lowest count detected in Ain Sokhna station (6 CFU /gm).The best marine sources of actinomycetes identified are sediments, from which their isolation is well Documented [13].The number and variety of actinomycetes present in any sample would be significantly influenced by geographical location, temperature; pH, organic matter content, agricultural activities, aeration, nutrient availability and moisture content [34].

Table 3: Physico-chemical parameters of sediment samples during winter, 2014

Sampling site	Physico-chemical parameters								
	Temp °C	pH	Salinity ‰	Dissolved oxygen (mg O ₂ /l)	Dissolved phosphate (µg at.PO ₄ -P /l)	Dissolved nitrate (µgat.NO ₃ N /l)	Dissolved nitrite (µg at. NO ₂ -N /l)	Dissolved ammonia (µg at. NH ₃ -N /l)	Organic matter (mg/l)
El-Tour	19.6	8.22	40.2	8.6	0.17	0.26	0.18	0.3	2.25
RasSidr	18.7	8.14	40.8	8.2	0.36	0.29	0.14	0.7	5.12
AdabiaHarbour	17.9	8.16	41.2	8.9	0.28	2.25	0.80	7.8	3.11
Suez North	17.6	8.14	41.7	8.8	0.17	18.15	0.77	15.0	2.63
Suez Middle	18.1	8.22	41.9	9.8	0.19	45.61	0.59	13.2	4.8
Ain Sokhna	18.1	8.24	41.8	8.6	0.14	0.27	0.09	4.8	0.71
RasGharib	18.9	8.20	40.4	9.9	3.88	2.20	2.22	47.2	7.12
RasShokair	19.2	8.25	41.1	8.9	0.28	0.12	0.15	0.9	4.51

Table 4: Actinomycets count (CFU /g) of sediment samples collected from Suez Gulf during winter, 2014.

Site	Count (CFU/gm)	Selected isolates
El-Tour	8	Isolates numbers 1- 4
RasSidr	15	isolates numbers 5 & 6
AdabiaHarbour	22	Isolates numbers 7 – 22
Suez North	20	Isolates numbers 23 – 28
Suez Middle	15	Isolates numbers 29-34
Ain Sokhna	6	Isolates numbers 35 & 36
RasGharib	18	Isolates number 37
RasShokair	15	Isolates number 38 – 41

3.3 Statistical Analysis

The stepwise multiple regression was applied to reflect the relationship between the environmental factors and the abundance of the recorded actinomycetes, the analysis illustrated that: the actinomycetes were affected by temperature and PO₄. The model equation was: Actinomycetes= 94.299 - 4.169 temp. - 2.239 PO₄. Aboulela *et al.*, [35] reported that, there was a highly significant relationship between total heterotrophs in sea

Water and water temperature, dissolved nitrate and nitrite. Variations in the organic contents, nutrients and the pollution levels led to variations in the density and frequency of bacteria between water and sediments.

3.4 Bioactivity of the Isolates

A total of 41 actinomycetes isolates were subjected to primary screening of their antagonistic effect against some bacterial pathogens. Only 11 showed antimicrobial activities against the bacterial pathogens *Bacillus subtilis* 6633, *Staphylococcus aureus* 25923, *Pseudomonas aeruginosa*

9027, *Bacillus cereus*, *Salmonella typhimurium* 14028, *Escherichia coli* 19404 and *Vibrio damsela*, the resulted inhibition zones were measured in terms of mean diameter of inhibition zones (mm) as recorded in (Table 5). Almost 80 % of the world's antibiotics are known to come from actinomycetes, mostly from the genera *Streptomyces* and *Micromonospora* [36]. Marine actinomycetes are particularly attractive because they have the high potency required for bioactive compounds to be effective in the marine environment, due to the diluting effect of sea water. Members of the actinomycetes, which live in marine environment, are poorly understood and only few reports are available. Actinomycetes represent attractive source for isolation of novel microorganisms and production of potent bioactive secondary metabolites [37].

3.5 Screening of Actinomycetes Isolates to Biosynthesis Metal Nanoparticles

3.5.1 Biosynthesis of Silver Nanoparticles

Isolates 13 and 38 showed ability to synthesis AgNPs at 1mM of silver nitrate and pH 8.5 after 5 days of incubation by color change from yellow to dark brown, (Table 6, Figure 2). While at concentrations of 0.5 and 2 mM AgNO₃, there was no color development. The absorption spectrum of the AgNPs showed a surface plasmon absorption band with a maximum of 410 nm, indicating the presence of AgNPs. The sharp narrow absorption peak located at 410nm for AgNPs was observed in the present study, (Figure 3) for strains 13 and 38, respectively. This was primarily observed by taking reading in UV-spectrophotometer at 410 nm in 1mM concentration as shown in (Table 7). The selected actinomycetes were

screened for antibacterial efficacy by agar well diffusion method, then we have investigated extracellular biosynthesis of silver nanoparticles of AgNO₃ as recommended by Deepa *et al.* [26]. The exact reaction mechanism leading to the biosynthesis of silver nanoparticles is believe that NADH-dependent reductase involving in reduction of silver ions [38]. Zeinat *et al.*, [39] recorded nearly result for this study, the absorption spectra of AgNPs synthesized by two *streptomyces* species showed a surface Plasmon absorption band with maximum of 417 nm indicating the resonance of AgNPs. This isolates 13 and 38 showed ability to synthesis AgNPs at 1mM of silver nitrate and pH 8.5 after 5 days of incubation by color change from yellow to dark brown, (Table 6, Figure 2). While at concentrations of 0.5 and 2 mM AgNO₃, there was no color development. The absorption spectrum of the AgNPs showed a surface plasmon absorption band with a maximum of 410 nm, indicating the presence of AgNPs. The sharp narrow absorption peak located at 410nm for AgNPs was observed in the present study, (Figure 3) for strains 13 and 38, respectively. This was primarily observed by taking reading in UV-spectrophotometer at 410 nm in 1mM concentration as shown in (Table 7). The selected actinomycetes were screened for antibacterial efficacy by agar well diffusion method, then we have investigated extracellular biosynthesis of silver nanoparticles of AgNO₃ as recommended by Deepa *et al.* [26]. The exact reaction mechanism leading to the biosynthesis of silver nanoparticles is believe that NADH-dependent reductase involving in reduction of silver ions [38]. Zeinat *et al.* [39] recorded nearly result for this study, the absorption spectra of AgNPs synthesized by two *streptomyces* species showed a surface Plasmon absorption band with maximum of 417 nm indicating the resonance of AgNPs. This observation is in good agreement with other studies [40,41].

Table 5: Inhibition zone (mm) of the isolates against some bacterial pathogens.

Pathogens	Isolate code										
	3	8	9	10	13	15	17	22	23	38	41
B. subtilis 6633	15.0	0.0	0.0	0.0	16.0	15.0	0.0	0.0	0.0	0.0	0.0
S. aureus 025923	0.0	0.0	0.0	12.0	18.0	0.0	0.0	0.0	0.0	15.0	0.0
P. aeruginosa 9027	0.0	0.0	0.0	0.0	0.0	0.0	0.0	0.0	0.0	0.0	22.0
B. cereus	0.0	0.0	0.0	0.0	14.0	12.0	0.0	0.0	0.0	0.0	0.0
S. typhimurium	20.0	15.0	16.0	14.0	16.0	18.0	25.0	15.0	0.0	15.0	15.0
E. coli 19404	0.0	0.0	0.0	0.0	16.0	0.0	0.0	0.0	20.0	16.0	0.0
V. damsela	18.0	20.0	10.0	13.0	0.0	0.0	18.0	0.0	0.0	0.0	

Table 6: Optimum conditions for silver nanoparticles detection (AgNO_3 concentrations and pH range) after 5 days of incubation -Ve (No change in color), +Ve (Changed color).

Strains	AgNO ₃ conc.	0.5 mM				1 mM				2 mM			
	pH	6.5	7.5	8.5	9.5	6.5	7.5	8.5	9.5	6.5	7.5	8.5	9.5
13		-Ve	-Ve	-Ve	-Ve	-Ve	-Ve	+Ve	-Ve	-Ve	-Ve	-Ve	-Ve
38		-Ve	-Ve	-Ve	-Ve	-Ve	-Ve	+Ve	-Ve	-Ve	-Ve	-Ve	-Ve

Table 7: UV spectrophotometer readings of AgNPs for supernatant of strains 13 and 38 after treatment with 1 mM of AgNO_3 .

Isolate code	Absorbance at 410 nm
13	0.376
38	0.355

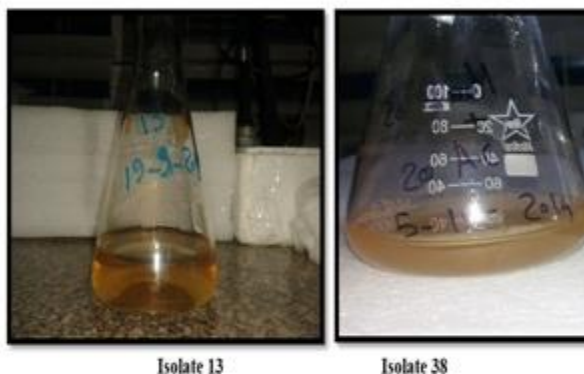
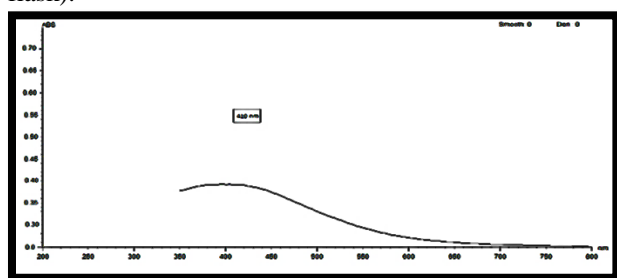
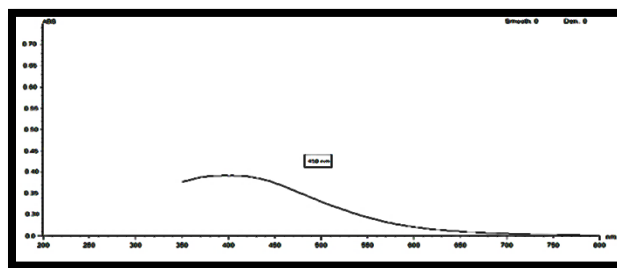


Fig.2: Cell filtrate of actinomycetes isolates (13 and 38) treated with (1Mm) at the beginning of incubation (right flask).



Isolate 13



Isolate 38

Fig. 3: UV-Vis absorption spectrum of Ag NPs synthesized by strain 13 and 38 after treated with 1mM AgNO_3 solution.

3.5.2 Biosynthesis of Gold Nanoparticles

Isolates 13 and 38 have ability to biosynthesis gold nanoparticles at 2 mM of HAuCl_4 and pH 4 after 4 h (Table 8). As shown in Figure 4, the visualized color of the solution changed from yellow to pink i.e. showed ability to synthesis gold nanoparticles. The formation of gold nanoparticles was monitored by UV-Visible spectroscopy by recording the spectra between 200-800 nm and simultaneously monitoring the appearance of the characteristic peak of gold nanoparticles at 530-550 nm using a double beam spectrophotometer (Figure 5). This was primarily observed by taking reading in UV-spectrophotometer as shown in (Table 9). Prakash *et al.*, [22] reported that, the reaction mixtures developed a range of colors within 2 h of incubation under different conditions indicating the synthesis of a variety of gold nanoparticles from *Streptomyces* sp. NK52. Also, Soltani *et al.*, [42] mentioned that, the use of *Streptomyces fulvissimus* isolate U in the extracellular synthesis of gold nanoparticles. Green synthesis of metal nano-particles using soil actinomycetes bacteria is an ecofriendly green process.

3.5.3 Biosynthesis of Zinc Nanoparticles

Only one isolate has the ability to synthesis zinc nanoparticles (Table 10). Primary confirmation for biosynthesis of zinc oxide nanoparticles from isolate 13 was recorded by visual observation, the color of the medium changed from yellowish to bright yellow. The characteristic surface showed plasmon absorption band with a maximum of 309 nm. Bright yellow color arises due to excitation of surface plasmon vibrations in the zinc nanoparticles. The reduction of zinc was subjected to analysis by using the UV-Vis spectrophotometer. Absorption spectra of Zn NPs formed in the reaction media

has absorbance peak at 309 nm by isolate 13 (Table 11 and Figure 6). In similar study; the biosynthetic route using *S. nematodiphila* (CAA) has been developed for the zinc sulfide nanoparticle production. During the visual observation, the color of the culture supernatant incubated with zinc sulfate changed from yellow to whitish yellow.

The appearance of a whitish Yellow color in the zinc sulfate-treated flask suggested the formation of zinc sulfide nanoparticles. The UV-Vis spectra were recorded broad peak which located between 380 to 400 nm and the strong absorbance centered at 390 nm [43].

Table 8: Optimum conditions for nanoparticles detection (HAuCl₄ concentrations and pH range) after 4h of incubation.

Strain	HAuCl ₄ Conc	0.5 mM				1 mM				2 mM			
	pH	4	5	6	7	4	5	6	7	4	5	6	7
13		-Ve	-Ve	-Ve	-Ve	-Ve	-Ve	-Ve	-Ve	+Ve	-Ve	-Ve	-Ve
38		-Ve	-Ve	-Ve	-Ve	-Ve	-Ve	-Ve	-Ve	+Ve	-Ve	-Ve	-Ve

Table 9: UV spectrophotometer readings of nanoparticles produced from different strains at 2 mM of HAuCl₄.

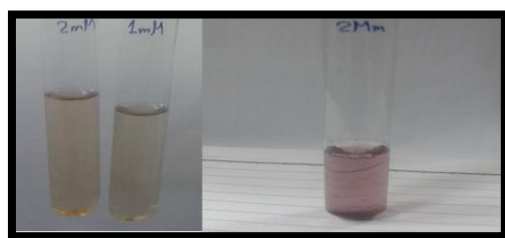
Isolate code	Absorbance
13	0.035
38	0.013

Table 10: Optimum conditions for nanoparticles detection (ZnSO₄ concentrations and pH range) after 24h of incubation.

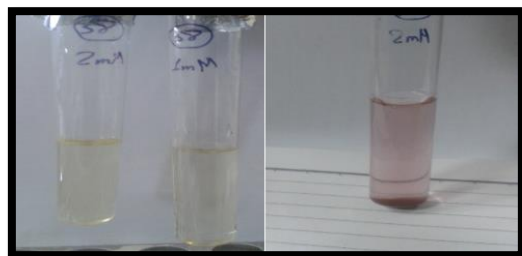
Isolate code	ZnSO ₄ conc.	50 mM				100 mM				150 mM			
	pH	4	5	6	7	4	5	6	7	4	5	6	7
13		-Ve	-Ve	-Ve	-Ve	-Ve	-Ve	-Ve	+Ve	-Ve	-Ve	-Ve	-Ve
38		-Ve	-Ve	-Ve	-Ve	-Ve	-Ve	-Ve	-Ve	-Ve	-Ve	-Ve	-Ve

Table 11: UV spectrophotometer readings of supernatant of isolates 13 at 100 mM ZnNP solution.

Isolate code	Absorbance
13	4.850

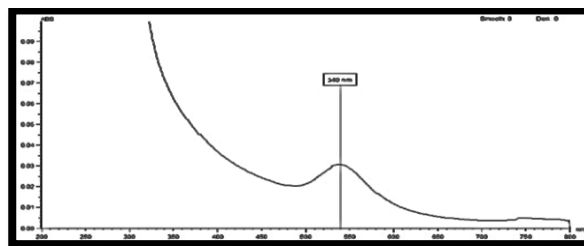


Isolate 13

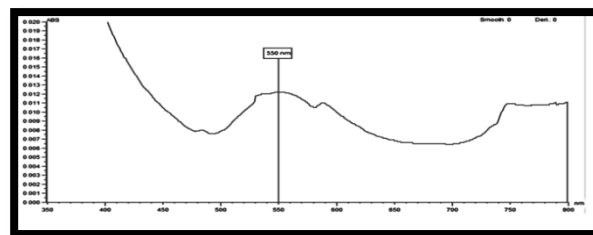


Isolate 38

Fig. 4: Cell filtrate of most isolates which treated with (2mM) of HAuCl₄ at the beginning of incubation and after 4h.

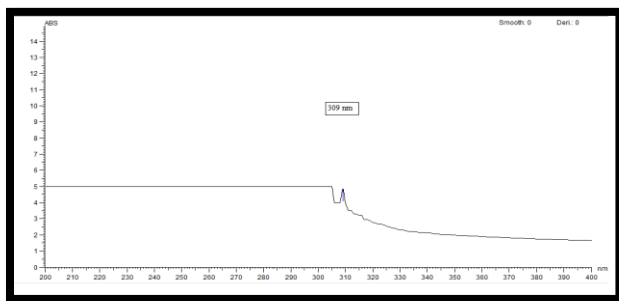


Isolate 13



Isolate 38

Fig. 5: UV-Vis absorption spectrum of AuNPs synthesized by strains (13 and 38) treated with 2mM HAuCl₄ solution.



Isolate 13

Fig. 6: UV-visible spectrum (Zn nanoparticles) by isolate 13 extract treated with 100 mM zinc sulfate.

3.6 Antibacterial Activity of Nano Particles Production

The antibacterial activity of silver nanoparticles which produced from isolates 13 and 38 were investigated against the previously used bacterial pathogens. Silver nanoparticles at 1mM concentration which produced from isolate 13 showed moderate activity against *Bacillus subtilis* 6633, *Staphylococcus aureus* 25923, *Pseudomonas aeruginosa* 9027 and *Salmonella typhimurium* 14028 (18mm), lower activity against *Bacillus cereus*, *Escherichia coli* 19404 and *Vibrio damsela* (16 mm). Silver nanoparticles from isolate 38 showed lower activities than that produced from isolate 13. The activities ranged from 13mm against *Vibrio damsela* to 18mm against *Staphylococcus aureus* 25923. No effect on two pathogens, *Pseudomonas aeruginosa* 9027 and *Escherichia coli* 19404. The biosynthesized AgNPs by both *Streptomyces* species proved effective against the tested bacteria but the inhibitory effect varied from one another. *Klebsiella*, *E. coli*, *Bacillus cereus*, and *S. aureus* were more affected by AgNPs compared to *Salmonella*, *Pseudomonas*, *Moraxella*, *Acinetobacter*, *Enterococcus*, and *S. pneumoniae* [39]. Also, Sadhasivam *et al.* [44] reported antimicrobial activity of biosynthesized AgNPs from *Streptomyces hygroscopicus* against *B. subtilis*, *E. coli*, *E. fecalis* and *C. albicans*. In another hand the antibacterial activity of gold nanoparticles which produced from strain 13 showed activity against *Staphylococcus aureus* 25923, *Salmonella typhimurium* 14028 and *Vibrio damsela* (16, 25 and 20 mm) respectively, while gold nanoparticles which produced from strain 38 affected on *Pseudomonas aeruginosa* 9027 and *Salmonella typhimurium* 14028 (23 and 20) respectively. Shahzadi *et al.*, [45] reported that, gold nanoparticles 6–40 nm in size exhibited high antibacterial activity, the mechanism of this activity was found to be size- and dose-dependent. It was more influential against Gram-negative bacteria. The antibacterial mechanism of AuNPs against four pathogenic bacteria demonstrated that AuNPs can be the next therapy against this enteric bacterium. In antibacterial activity testing by well-diffusion method, the actinomycete biomass exposed to H₂AuCl₄ showed inhibition zone size of 14 and

20 mm against *S. aureus* and *E. coli*, respectively, but the untreated actinomycete biomass showed no inhibition [46].

Zinc nanoparticles produced from isolate 13 showed reasonable activity against only *Escherichia coli* 19404 (36 mm) and *Salmonella typhimurium* 14028 (34 mm) and no effect on the other pathogens. Noor & Halah [47] reported that, zinc oxide nanoparticles had strong antibacterial activity and could inhibit one of the most important pathogenic bacteria *P. aeruginosa*.

3.7 Molecular Phylogeny of the Selected Isolates

Based on the obtained results, actinomycetes isolates 13 and 38 were selected for identification and molecular phylogenetic analysis. Phylogenetic analysis based on 16S rDNA sequence comparison for establishing phylogenetic and evolutionary relationships among organisms [34]. Genomic DNA was prepared, and the gene coding for 16S rRNA was partially amplified using the universal primers

Primers	Sequence (5' to 3')
16S 27F	AGAGTTTGATCCTGGCTCAG
16S 1492R	GGTACCTTGTTACGACTT

The produced amplicons of the selected isolate were detected using agarose gel electrophoresis as shown in Figure 7.

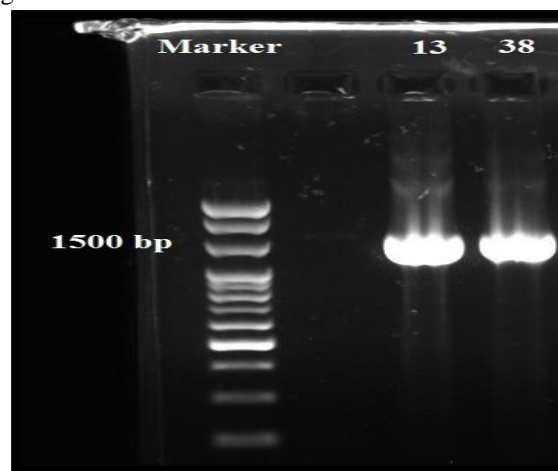


Fig. 7: Agarose gel electrophoreses of the amplified 16S rRNA gene of isolates 13 and 38.

The sequencing data utilizing this strategy (ABI 3730x1) was 1500 base pair. as shown in (figure 7). This sequence was aligned with other sequences of related actinomycetes on the database to determine its phylogenetic relationship to other actinomycetes. According to 16S rRNA gene sequence analysis of isolates 13 and 38 compared with those which gave the highest homology using Blast search computer based program. The resulting data indicated that, the isolates 13 was similar to *Streptomyces rochei* with 99 %

similarity percentage and the isolate 38 similar to *Streptomyces* sp. with 91% similarity percentage. The sequence of strain 13 was deposited in Gene-Bank as *Streptomyces rochei* HMM13 with accession number KR108310, and strain 38 deposited in Gene-Bank as *Streptomyces* sp. MHM38 with accession number KU764745 and the phylogenetic tree was constructed as shown in (Figure 8 and 9). Several studies reported the potential of *Streptomyces* sp. in biosynthesis of silver nanoparticles [48,49,50].

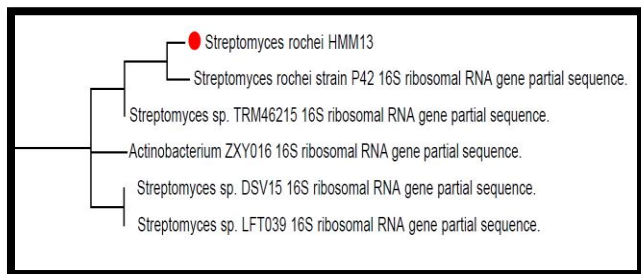


Fig. 8: Phylogenetic tree of *Streptomyces rochei* HMM13 based on partial sequencing of 16S rRNA.

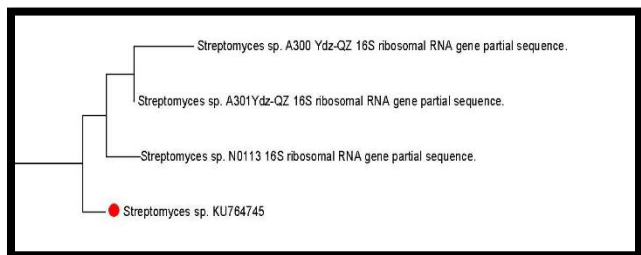


Fig.9: Phylogenetic tree of *Streptomyces* sp. MHM38 based on partial sequencing of 16S rRNA.

3.8 Characterization of Silver Nanoparticles Synthesized by *Streptomyces Rochei* HMM13

The biosynthesized AgNPs were achieved by addition of silver nitrate (1mM) to the culture supernatant and monitored by color change after incubation then confirmed by UV-Visible spectrophotometer, X-ray, Fourier transform-infrared spectroscopy and scanning electron microscopy. The results of characterization were reported in previous study by Abd-Elnaby *et al.*, [51], where, the obtained AgNPs are spherical in shape with a particle size of 22–85 nm.

3.9 Optimization of the Culture Conditions for *Streptomyces Rochei* HMM13 by Plackett–Burman Design

Plackett-Burman design has been employed to evaluate the significant effect of starch nitrate agar medium components for production of silver nanoparticles by *Streptomyces rochei* HMM13 and application of AgNPs as antibacterial agent against, *Salmonella typhimurium* 14028, *Escherichia*

coli 19404, and *Vibrio damsela*. Statistical experimental designs are powerful tools for searching the key factors rapidly form a multivariable system and minimizing the error in determining the effect of parameters and the results are achieved in an economical manner [52]. The experimental results of the applied Plackett-Burman design for seven cultural variables against *S. typhimurium* 14028 was illustrated in (Tables 12).

Statistical analysis of the data (t-test) showed that, among the examined environmental factors, Starch, MgSO₄·7H₂O, KNO₃ and temperature were the most significant independent variable that affects the nanoparticles production and consequently, the inhibition zone diameter against *S. typhimurium* 14028 (Table 13).

The main effects of the examined factors on the inhibition zone diameter were calculated and represented in Figure 10. Based on these results, the positive (+) level of starch, KNO₃, K₂HPO₄ and pH, in addition to the negative level (-) of MgSO₄·7H₂O, FeSO₄ and temperature supported the production. Moreover, the *t*-value represented in Table 14 supports this observation. Interaction of starch and MgSO₄·7H₂O, increase the inhibition zone diameter. This approach verified the validity of the applied design. A verification experiment was applied to evaluate the basal versus the optimized medium.

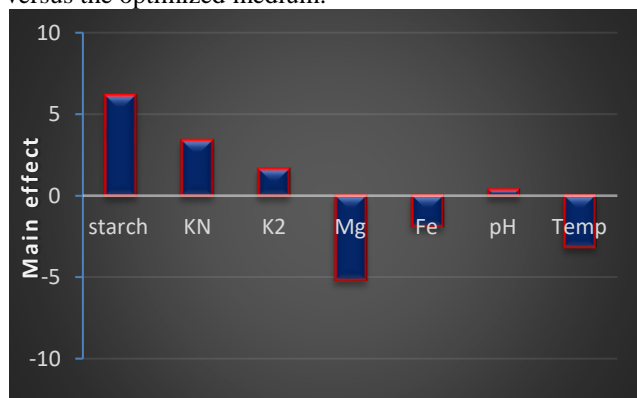


Fig. 10: Elucidation of fermentation conditions affecting the production of AgNPs by *Streptomyces rochei* HMM13 against *Salmonella typhimurium* 14028.

Verification experiment: A verification experiment was applied to evaluate the basal versus the optimized medium. Data in (Table 14) and Figure 11 showed that about 22 (mm) inhibition zone diameter after incubation with 1.2 fold increase when compared to the control basal medium 18 (mm), on another hand, the uv spectrophotometer reading from verified medium showing rise up to 0.435 nm compared with the control basal medium 0.376nm (1.16 fold increase). The composition of the verified medium as follows (g/l): Starch, 30g; KNO₃, 1.5g; K₂HPO₄, 0.75g; MgSO₄·7H₂O, 0.25g; FeSO₄, 0.005; pH, 6 and Temperature 33°C. The experimental results of the applied Plackett-Burman design for seven cultural variables against *E. coli* 19404 were illustrated in Tables 15.

Table12: The experimental results of the applied Plackett-Burman design for seven cultural variables (application on *S. typhimurium* 14028).

Trial	Starch	KN	K ₂	Mg	Fe	pH	Temp	Abs.	AgNPs inhibition zone (mm) Against <i>S. typhimurium</i>
1	-	-	-	+	+	+	-	0.177	0
2	+	-	-	-	-	+	+	0.340	20
3	-	+	-	-	+	-	+	0.230	10
4	+	+	-	+	-	-	-	0.430	22
5	-	-	+	+	-	-	+	0.210	0
6	+	-	+	-	+	-	-	0.380	25
7	-	+	+	-	-	+	-	0.455	24
8	+	+	+	+	+	+	+	0.380	16
9	0	0	0	0	0	0	0	0.298	16

Table 13: Statistical analyses of the Plackett-Burman experimental results.

Variable	Main effect	t-value*
Starch	6.12	13.36
KNO ₃	3.37	7.36
K ₂ HPO ₄	1.62	3.54
MgSO ₄ .7H ₂ O	-5.12	-11.18
FeSO ₄	-1.87	-4.09
pH	0.37	0.81
Temperature	-3.12	-6.81

Table14: A verification experiment: Inhibition zone of silver NPs produced from *S. rochei*HMM13 against *S. typhimurium* 14028 grown on basal versus verified medium.

Medium	Inhibition zone (mm)	Abs. at 410nm
Basal medium with AgNO ₃	18	0.376
Verified medium with AgNO ₃	22	0.435

Table 15: The experimental results of the applied Plackett-Burman design for seven cultural variables (application on *E. coli* 19404)

Trial	Starch	KN	K ₂	Mg	Fe	pH	Temp	Abs.	AgNPs Inhibition (mm) <i>E. coli</i> 19404
1	-	-	-	+	+	+	-	0.210	0
2	+	-	-	-	-	+	+	0.380	20
3	-	+	-	-	+	-	+	0.240	10
4	+	+	-	+	-	-	-	0.470	20
5	-	-	+	+	-	-	+	0.270	0
6	+	-	+	-	+	-	-	0.480	20
7	-	+	+	-	-	+	-	0.410	20
8	+	+	+	+	+	+	+	0.430	0
9	0	0	0	0	0	0	0	0.320	16



Fig. 11: Inhibition zone diameter of Ag NPs of *S.rochei* HMM13 grown on verified medium against *S. typhimurium* 14028.

Statistical analysis of the data (t- test) showed that, among the examined environmental factors, $MgSO_4 \cdot 7H_2O$, temperature, starch and $FeSO_4$ was the most significant independent variable that affect the suppression percentage of *Escherichia coli* 19404 (Table16).

Table 16: Statistical analyses of the Plackett-Burman experimental results.

Variable	Main effect	t-value*
Starch	3.75	1.0
KNO_3	1.25	0.33
K_2HPO_4	-1.25	-0.33
$MgSO_4 \cdot 7H_2O$	-6.25	-1.66
$FeSO_4$	-3.75	-1.0
pH	-1.25	-0.33
Temperature	-3.75	-1.0

The main effects of the examined factors on the inhibition zone diameter were calculated and represented in Figure 12. Based on these results, the positive level (+) of starch and KNO_3 and the negative (-) level of the other variables supports the production. Moreover the *t*-value represented in Table 16 supports this observation.

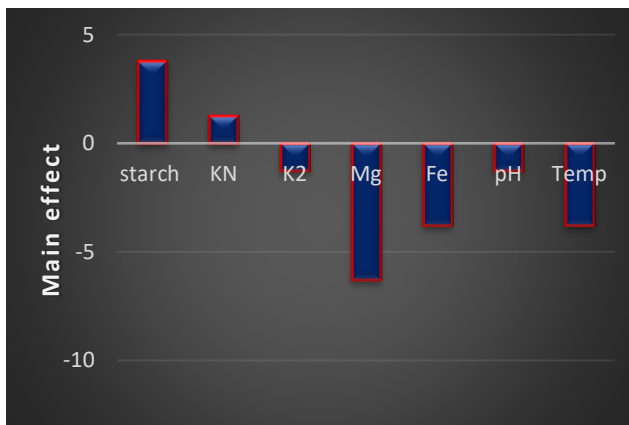


Fig. 12: Elucidation of fermentation conditions affecting the production of AgNPs by *Streptomyces rochei* HMM13 against *Escherichia coli* 19404.

Verification experiment: A verification experiment was applied to evaluate the basal versus the optimized medium. Data in Table 17 showed that about 20 (mm) inhibition zone diameter with 1.25 fold increase when compared to the control basal medium 16 (mm), Figure 13 was achieved the UV spectrophotometer readings from verified medium showing rise up to 0.487 nm i.e. 1.13 fold increase compared with the control basal medium (0.376 nm). The composition of the verified medium as follows (g/l): Starch, 30g; KNO_3 , 1.5g; K_2HPO_4 , 0.75g; $MgSO_4 \cdot 7H_2O$, 0.25g; $FeSO_4$, 0.005; pH, 6 and temperature $33^\circ C$.

Table17: A verification experiment: Activity of silver NPs production from *S. rochei* HMM13 against *Escherichia coli* 19404 grown on basal versus verified medium.

Medium	Inhibition zone (mm)	Abs. at 410 nm
Basal medium with $AgNO_3$	16	0.376
Verified medium with $AgNO_3$	20	0.487

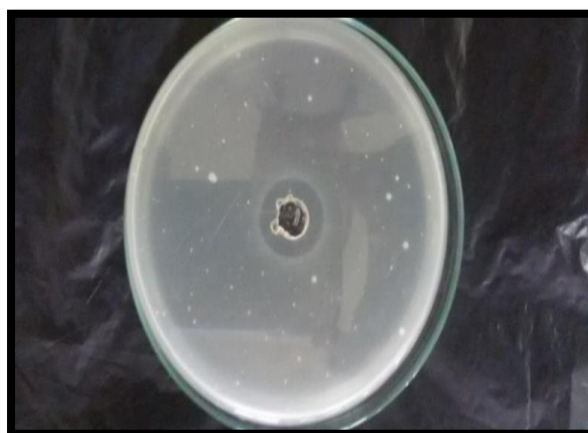


Fig. 13: Inhibition zone diameter of Ag NPs of *S.rochei* HMM13 grown on verified medium against *Escherichia coli* 19404.

The experimental results of the applied Plackett-Burman design for seven cultural variables against *Vibrio damsela* was illustrated in (Table18)

Statistical analysis of the data (t- test) showed that, among the examined environmental factors, starch was the most significant independent variable that affect the suppression percentage of *Vibrio damsela* (Table 19).

The main effects of the examined factors on the inhibition zone diameter were calculated and represented in Figure 14. Based on these results, the positive (+) level of all variables supports the production except $MgSO_4 \cdot 7H_2O$, $FeSO_4$ and temperature which must be taken with (-) levels. Moreover, the *t*-value represented in Table 19 supports this observation.

Table 18: The experimental results of the applied Plackett-Burman design for seven cultural variables (Application on *Vibrio damsela*)

Trial	ST	KN	K ₂	Mg	Fe	pH	Tem	Abs.	AgNPs inhibition zone (mm) against <i>Vibrio damsela</i>
1	-	-	-	+	+	+	-	0.270	0
2	+	-	-	-	-	+	+	0.450	24
3	-	+	-	-	+	-	+	0.310	0
4	+	+	-	+	-	-	-	0.470	24
5	-	-	+	+	-	-	+	0.288	0
6	+	-	+	-	+	-	-	0.490	25
7	-	+	+	-	-	+	-	0.476	22
8	+	+	+	+	+	+	+	0.360	15
9	0	0	0	0	0	0	0	0.326	13

Table 19: Statistical analyses of the Plackett-Burman experimental results.

Variable	Main effect	t-value*
Starch	8.25	33.0
KNO ₃	1.5	6.0
K ₂ HPO ₄	1.75	7.0
MgSO ₄ .7H ₂ O	-4.0	-16.0
FeSO ₄	-3.75	-15.0
pH	1.5	6.0
Temperature	-4.0	-16.0

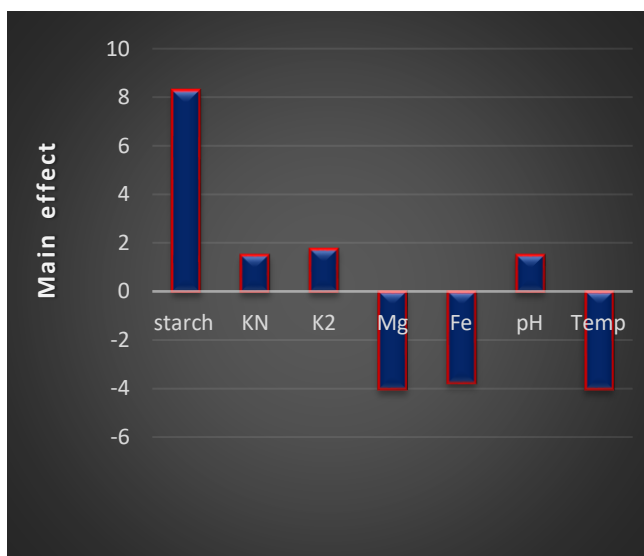


Fig. 14: Elucidation of fermentation conditions affecting the production of AgNPs by *Streptomyces rochei*HMM13 against *Vibriodamsel*.

Verification experiment: A verification experiment was applied to evaluate the basal versus the optimized medium. Data in (Table 20) shows that about 19 (mm) inhibition

zone diameter achieved with 1.19 fold increase when compared to the control basal medium 16 (mm) Figure 15. The UV spectrophotometer readings from verified medium showed that 0.497 nm about (1.32 fold increase) compared with the control basal medium 0.376 nm was detected. The composition of the verified medium as follows (g/l): Starch, 30g; KNO₃, 1.5g; K₂HPO₄, 0.75g; MgSO₄.7H₂O, 0.25g; FeSO₄, 0.005; pH, 8 and temperature 33°C.

Table 20: A verification experiment: Inhibition zone of silver NPs produced from *S. rochei*HMM13 against *Vibrio damsela* grown on basal versus verified medium.

Medium	Inhibition zone (mm)	Abs at 410 nm
Basal medium with AgNO ₃	16	0.376
Verified medium with AgNO ₃	19	0.497

El-Naggaret *et al.*, [53] reported, statistical optimization of fermentation conditions using Plackett-Burman design and Box-Behnken design appears to be a valuable tool for the production of AgNPs by *Streptomyces carbonensis* SSHH-1E, about 4.5 fold increase in AgNPs production was achieved with the following optimized factors: inoculum

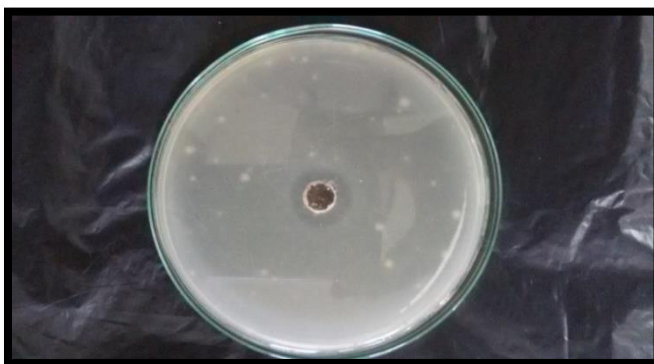


Fig. 15: Inhibition zone diameter of Ag NPs of *S. rochei* HMM13 grown on verified medium against *Vibrio damsela*.

age (48 h), peptone (0.5 g/L), and pH value (8). Statistical optimization of fermentation conditions using Plackett-Burman design and Box-Behnken design appears to be a valuable tool for the production of AgNPs by *Streptomyces viridodiataticus* SSHH-1. Initial screening of production parameters was performed using a Plackett-Burman design and the variables with statistically significant effects on AgNPs production were identified. Among the 14 variables tested, inoculum age, medium volume, and peptone concentration were identified as the most significant factors for AgNPs production (confidence level above 99%). These variables were selected for further optimization studies using a Box-Behnken design. The statistical optimization by RSM resulted in a 4.43-fold increase in the production of AgNPs by *Streptomyces viridodiataticus* [12].

4 Conclusions

Streptomyces rochei HMM13 is an excellent microbial resource for the synthesis of AgNPs. The surface plasmon resonance band at 400 nm in UV-visible spectrum indicates the primary evidence for synthesis of AgNPs. Statistical optimization of fermentation conditions using Plackett-Burman design appears to be a valuable tool for the production of AgNPs by *Streptomyces rochei* HMM13.

References

- [1] R. Montaser and H. Luesch. Marine natural products: A new wave of drugs. *Future Medicinal Chemistry*, **3**, 1475–1489 (2011).
- [2] A. Choudhary, L.M. Naughton, I. Montánchez, A.D.W. Dobson and D.K. Rai. Current Status and Future Prospects of Marine Natural Products (MNP) as Antimicrobials. *Marine Drugs*, **15**(9), 272 (2017).
- [3] C. Sharma, P. Mehtani, P. Bhatnagar and N. Mathur. Saline waters: A potential source of actinomycetes possessing antibacterial activity. *International Journal of Pharmacy and Biological Sciences*, **3**, 242–251 (2013).
- [4] S. Mathur and C. Hoskins. Drug development: lessons from nature. *Biomed Rep.*, **6**(6), 612–614 (2017).
- [5] Z. Cwala, E.O. Lgbinsosa and A.X. Okoh. Assessment of antibiotics production potentials in four actinomycetes isolated from aquatic environments of the Eastern Cape Province of South Africa. *African J. Pharmacy Pharmacology*, **5**(2), 118–124 (2012).
- [6] J. Berdy. Bioactive microbial metabolites. *Journal of Antibiotics*, **58**(1), 1–26 (2005).
- [7] J.S. Kim. Antibacterial activity of Ag⁺ ion-containing silver nanoparticles prepared using the alcohol reduction method. *J. Ind. Eng. Chem.*, **13**(5), 718–722 (2007).
- [8] K.S. Siddiqi, A. Husen and R.A.K. Rao. A review on biosynthesis of silver nanoparticles and their biocidal properties. *J. Nanobiotechnology*, **16**, 14 (2018).
- [9] S. Pradhan. Comparative analysis of silver nanoparticles prepared from different plant extracts (*Hibiscus rosa sinensis*, *Moringa oleifera*, *Acorus calamus*, *Cucurbita maxima*, *Azadirachta indica*) through green synthesis method. MSc. thesis. National Institute of Technology, Rourkela, (2013).
- [10] N.I. Hulkoti and T. Taranath. Biosynthesis of nanoparticles using microbes—A review. *Colloids and Surfaces. Biointerfaces*, **121**, 474–483 (2014).
- [11] N.E.A. El-Naggar and N.A. Abdelwahed. Application of statistical experimental design for optimization of silver nanoparticles biosynthesis by a nanofactory *Streptomyces viridochromogenes*. *J. Microbiol.*, **52**(1), 53–63 (2014).
- [12] A. Mohamedin, E. El-Naggar, N. Hamza, and A.A. Sherief. Green synthesis, characterization and antimicrobial activities of silver nanoparticles by *Streptomyces viridodiataticus* SSHH-1 as a living nanofactory: Statistical optimization of process variables. *Curr. Nanoscience*, **11**, 5 (2015).
- [13] G.M. Abou-elela. Studies on actinomycetes in marine water and sediments of Alexandria beaches, (Egypt). Ph.D. thesis, Fac. Sci., Alex. Univ., (1999).
- [14] P.R. Jensen, R. Dwight and W. Fenical. Distribution of actinomycetes in near shore tropical marine sediments. *Appl. Environ. Microbiol.*, **57**, 1102–1108 (1991).
- [15] L.S. Clesceri, A.E. Greenberg and A.D. Eaton. *Standard Methods for Determination of Wastewater*, (22 ed.), American Public Health Association, Washington D.C., USA, (2012).
- [16] K. Grasshoff. *Methods of sea water analysis*. Weinheim (ed.), New York; Verlag Chemie., 317 (1976).
- [17] J.D.H. Strickland and T.R.A. Parsons. *Practical handbook of sea water analysis*. Fish Res. Bd. Canad., 311 (1968).
- [18] F. Koroleff. Determination of ammonia as indophenol blue. *International Council for the Exploration of the Sea (ICES)*, **8** (1969).
- [19] M.M. Ellis, B.A. Westfall and D.M. Ellis. Determination of water quality. *Int. Fish & Wild Life Ser. Res. Report.*, **9**, 122 (1946).
- [20] P. Selvakumar, S. Viveka, S. Prakash, S. Jasminebeaula and R. Uloganathan. Antimicrobial activity of extracellularly synthesized silver nanoparticles from marine derived *Streptomyces rochei*. *Int. J. Pharma. biological sci.*, **3**, 188–197 (2012).
- [21] S. Priyagarini, S. Sathishkumar and K. Bhaskararao. Biosynthesis of silver nanoparticles using actinobacteria and evaluating its antimicrobial and cytotoxicity activity. *Int. J. Pharma. Pharma. Sci.*, **5**(2), 709–712 (2013).
- [22] D. Prakash, V. Mahale, A. Bankar, N. Nawani, S. Zinjarde and B. Kapadnis. Biosynthesis of colloidal gold

- nanoparticles by *Streptomyces* sp. NK52 and its anti-lipid peroxidation activity. *Indian J. Experimental Biol.*, **51(11)**, 969-972 (2013).
- [23] C.R. Kelmani, C. Ashajyothi, Manjunath, and N. Rahul, Antibacterial activity of biogenic zinc oxide nanoparticles synthesised from *Enterococcus faecalis*. *Int. J. Chemtech Res.*, **6**, 3131-3136 (2014).
- [24] Singh D., Rathod V., Fatima L., Kausar A., Vidyashree N.A. and Priyanka B. Biologically reduced silver nanoparticles from *Streptomyces* sp. VDP-5 and its antimicrobial efficiency. *Int. J. Pharma. Sci. Res.*, **4(2)**, 31-36.
- [25] D.G. Yablon, J. Grabowski and I. Chakraborty, Measuring the loss tangent of polymer materials with atomic force microscopy based methods. *Measurement Sci. Technol.*, **25(5)**, 055-402 (2014).
- [26] S. Deepa, K. Kanimozhi and A. Panneerselvam. Antimicrobial activity of extracellularly synthesized silver nanoparticles from marine derived actinomycetes. *Int. J. Current Microbiol. Appl.*, **2(9)**, 223-230 (2013).
- [27] T.A. Hall. Bio-Edit: a user-friendly biological sequence alignment editor and analysis program for Windows 95/98/NT. *Nucl. Acids Symp. Ser.*, **4**, 95-98 (1999).
- [28] R.L. Plackett and J.P. Burman. The design of optimum multifactorial experiments. *Biometrika.*, **33(4)**, 305-325 (1946).
- [29] W.G. Cochran and G.W. Snedecor. *Statistical Methods*. Iowa State University Press, Ames (IA), USA, (1989).
- [30] M.A. Hamed. Determination of some microelements in the aquatic ecosystem and their relation to the efficiency of aquatic life. Ph.D. Thesis, Faculty of . Sci. Mansoura Univ., (1996).
- [31] J.P. Riley and G. Skirrow: *Chemical Oceanography*. Vol. 1 & 2. - London and New York: Academic Press., 1965. 147 (1967).
- [32] M. Fahmy, M. Sheriadah, A. Aboul Soeud, S. Abdel Rahman, and M. Shindy. Hydrography and chemical characteristics of the coastal water along the Gulf of Suez. *Egypt. J. Aqua. Res.*, **31**, 1-14 (2005).
- [33] WHO, World health organization. Nitrate, Nitrite and Nitrosocompounds. Geneva. Environmental health criteria., 5 (1978).
- [34] K. Isik, T. Gencbay, F. Özdemir-Kocak and E. Cil. Molecular identification of different actinomycetes isolated from East Black Sea region plateau soil by 16S rDNA gene sequencing", *African J Microbiol. Res.*, **8(9)**, 878-887 (2014).
- [35] G.M. Abou-elela, N.B. Ghanem and M. Okbah. Occurrence and distribution of some actinomycetes groups in Burullous Lake. *Bull. Fac. Sci. Assuit Univ.*, **33(2-d)**, 133-146, (2004).
- [36] G. Oza, S. Pandey, R. Shah and M. Sharon. Extracellular fabrication of silver nanoparticles using *Pseudomonas aeruginosa* and its antimicrobial assay. *Advanc. Appl. Sci. Res.*, **3**, 1776-1783 (2012).
- [37] Y. Usha, S. Koppula and Z. Vishnuvardhan. Bioactive metabolites from marine sediments (*Streptomyces* species) of three coastal areas. *Drug Invention Today.*, **2(6)**, 114-117 (2011).
- [38] A.I. El-Batal, A.M. Hashem and N.M. Abdelbaky, Gamma radiation mediated green synthesis of gold nanoparticles using fermented soybean-garlic aqueous extract and their antimicrobial activity. *Springer Plus.*, **2**, 129 (2013).
- [39] K. Zeinat, S. Mahmoud, and E.N. Noha Biosynthesis, Characterization, and Antimicrobial Activity of Silver Nanoparticles from Actinomycetes. *Res. J. . Biol. Chem. Sci.*, **7(1)**, 0975-8585 (2016).
- [40] N. Duran, P.D. Marcato, G.I.H. De Souza, O.L. Alves and E. Esposito. Antibacterial effect of silver nanoparticles produced by fungal process on textile fabrics and their effluent treatment. *J. Biomed. Nanotechnology.*, **3**, 203-208 (2007).
- [41] N. Vigneshwaran, N.M. Ashtaputre, P.V. Varadarajan, R.P. Nachane, K.M. Paralikar, and R.H. Balasubramanya. Biological synthesis of silver nanoparticles using the fungus *Aspergillus flavus*. *Materials Letters.*, **61**, 1413-1418 (2007).
- [42] N.M. Soltani, B.G.H. Shahidi and N. Khaleghi. Biosynthesis of gold nanoparticles using *Streptomyces fulvissimus* isolate. *Nanomedicine.*, **2(2)**, 153 -159 (2015).
- [43] M. Chelladurai and A. Gurusamy. A novel biological approach on extracellular synthesis and characterization of semiconductor zinc sulfide nanoparticles. *Nanoscience.*, **5**, 389-395 (2013).
- [44] S. Sadhasivam, P. Shanmugam and K. Yun. Biosynthesis of silver nanoparticles by *Streptomyces hygroscopicus* and antimicrobial activity against medically important pathogenic microorganisms. *Colloids and Surfaces B: Biointerfaces.*, **81(1)**, 358-362 (2010).
- [45] S. Shahzadi, Z. Noshin, R. Saira, S. Rehana, N. Jawad and N. Shahzad Gold nanoparticles: an efficient antimicrobial agent against enteric bacterial human pathogen. *Nanomaterials.*, **6**, 71, (2016).
- [46] R. Balagurunathan, M. Radhakrishnan, Babu, R. Rajendran and D. Velmurugan. Biosynthesis of gold nanoparticles by actinomycete *Streptomyces viridogens* strain HM10. *Indian J. Biochem. Biophy*, **48(5)**:331, (2011).
- [47] H.A. Noor and D.S. Halah. Antibacterial activity of modified zinc oxide nanoparticles against *Pseudomonas aeruginosa* isolates of burn infections. *World Scientific News.*, **33**, 1-14 (2016).
- [48] A. Samundeeswari, S. Priya Dhas, J. Nirmala, S.P. John, A. Mukherjee and N. Chandrasekaran. Biosynthesis of silver nanoparticles using actinobacterium *Streptomyces albobriseolus* and its antibacterial activity. *Biotechnol. Appl. Biochem.*, **59 (6)**, 503-507 (2012).
- [49] R. Chauhan, A. Kumar and J. Abraham. Biological approach to the synthesis of silver nanoparticles with *Streptomyces* sp JAR1 and its antimicrobial activity. *Sci. Pharm.*, **81(2)**, 607-621 (2013).
- [50] R.S. Prakasham, B.S. Kumar, Y.S. Kumar and K.P. Kumar. Production and characterization of protein encapsulated silver nanoparticles by marine isolate *Streptomyces parvulus* SSNP11. *Indian J. Microbiol.*, **54 (3)**, 329-336 (2014).
- [51] H.M. Abd-Elnaby, G.M. Abo-Elala, U.M. Abdel-Raouf and M.H. Hamed. Antibacterial and anticancer activity of extracellular synthesized silver nanoparticles from marine *Streptomyces rochei* MHM13. *Egypt. J. Aqua. Res.*, **42**, 301-312 (2016).
- [52] C. Xiong, W. Jinhua, and L. Dongsheng. Optimization of solid-state medium for the production of inulinase by *Kluyveromyces 5120* using response surface methodology. *Biochem. Eng. J.*, **34**, 179-184 (2007).
- [53] El-Naggar N.E., Mohamedin A., Hamza S.S. and Sherief A. Extracellular Biofabrication, Characterization, and Antimicrobial Efficacy of Silver Nanoparticles Loaded on Cotton Fabrics Using Newly Isolated *Streptomyces* sp. SSHH-1E. *J. Nanomaterials*, (2016).

Gehan Abo-elelais Professor of marine microbiology at National Institute of Oceanography and Fisheries, Egypt. Her work focused on marine environment and especially bioactive compounds from marine actinomycetes.

She was the head of marine microbiology lab.– Environment Division at National Institute of Oceanography and Fisheries. Number of her publication exceeded than 33.

Hanan M. Abd-Elnaby is Professor of marine microbiology at National Institute of Oceanography and Fisheries, Egypt. She received the Ph.D. degree in Environmental Studies at Institute of Graduate Studies and Research, Alexandria University, Egypt.

She is referee and Editor of some international journals in the frame of microbiology and biotechnology. Her main research interests are: biodegradation of hydrocarbons, bioaccumulation of heavy metals, production of bioactive natural products from microbes and marine resources and their applications, using probiotic bacteria to improve water quality against pathogens in aquacultures and biosynthesis of metal nanoparticles.

Usama Abd-Elraoufi is professor of botany and microbiology department and the Vice University President, Al-Azhar University, Assuit Branch, Egypt.

Moaz. M. Hamed Ph.D. in Microbiology Faculty of Science, Al-Azhar University- Assuit Branch, Egypt.

Lecturer in Microbiology Dept., Marine Environment Division, National Institute of Oceanography and Fisheries, Suez and Aqaba branch, Egypt. publication exceeded than 33.